THE JOURNAL OF PHYSICAL CHEMISTRY B

Article

pubs.acs.org/JPCB

Behavior of Platelet Activating Factor in Membrane-Mimicking Environment. Langmuir Monolayer Study Complemented with Grazing Incidence X-ray Diffraction and Brewster Angle Microscopy

Michał Flasiński,* Marcin Broniatowski, Paweł Wydro, Katarzyna Hąc-Wydro, and Patrycja Dynarowicz-Łątka

Faculty of Chemistry, Jagiellonian University, Ingardena 3, 30-060 Kraków, Poland

Supporting Information

ABSTRACT: 1-*O*-Octadecyl-2-acetyl-*sn*-glycero-3-phosphocholine (PAF) belonging to the class of single-chained ether phospholipids is widely known from its essential biological activities. There is a growing body of evidence that some significant aspects of PAF actions are connected with its capability to direct intercalation into biomembranes' environment. Although this mechanism is of great importance in the perspective of understanding PAF implications in various physiological processes, in the literature, there is a lack of studies devoted to this subject. It is still unknown which is the exact influence of membrane composition, molecular organization, and its other properties on the PAF impact on cells and tissues. Unfortunately, the biological studies carried out on cell cultures do not provide satisfactory results, mainly because of the complexity of natural systems. In order to obtain insight into the behavior of PAF in a lipid environment at the molecular level, the application of appropriate model systems is required. Among them, Langmuir monolayers are very often applied as a simple but very efficient platform for studies of the interactions between membrane lipids. In the present paper, special attention is focused on the issue concerning the interactions between PAF and two representatives of membrane components occurring mainly in the outer leaflet of natural bilayers, namely, cholesterol and DPPC. The application of Langmuir monolayers enabled us to construct the effective model mimicking the exogenous incorporation of PAF into membrane environment. On the basis of the obtained results, a thorough discussion was carried out and the conclusions derived from the traditional thermodynamic analysis were confronted with microscopic analysis of surface domains and the GIXD results. The selection of experimental techniques enables us to obtain information regarding the miscibility and interactions in the binary mixed films as well as the molecular organization of film-forming molecules on water surface. The experiments revealed that the addition of the investigated single-chained ether phospholipid into both cholesterol and DPPC monolayers causes a considerable decrease of monolayer condensation. On the basis of thermodynamic analysis, it was found that PAF mixes and consequently interacts strongly with cholesterol, whereas its interactions with DPPC are thermodynamically unfavorable. Differences between the PAF influence on cholesterol and DPPC monolayer found its corroboration in the results obtained with the GIXD technique. Namely, the monolayer of DPPC can incorporate more PAF than the model membrane containing cholesterol. The obtained results indicate that short chained *sn*-2 ether phospholipid is able to modify model membrane properties in a concentration-dependent way.

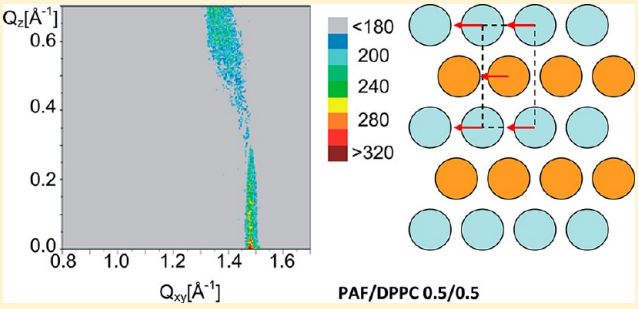

INTRODUCTION

Ether phospholipids constitute a class of biologically important molecules, which fulfill various structural and signaling functions in living organisms.[1] Among this group, a broad range of structurally differing compounds can be found; thus, both the properties and activities that they demonstrate vary significantly.[2] One of the main subclasses includes the single-chained ether lipids represented by 1-*O*-alkyl-2-acetyl-*sn*-glycero-3-phosphocholines. These physiologically active phospholipids, widely known as platelet activating factor (PAF) or PAF-acether, were discovered in the early 1970s by Benveniste and co-workers.[3] Originally, PAF was named after its first recognized property, i.e., its tendency to platelet aggregation;[4] however, it is well established that this function represents only an example of PAF's manifold activities. In fact, the term *platelet activating factor* refers traditionally to the family of structurally related phospholipids bearing an acetyl moiety in the *sn*-2 position of the glycerol backbone but differing in the length and saturation of the second alkyl chain attached via the ether linkage.[5] It is, however, noteworthy that naturally occurring PAF possesses a predominantly fully hydrogenated chain of 18 or 16 carbon atoms.[6] It was proved that PAF is

Received: March 27, 2012
Revised: July 8, 2012
Published: July 26, 2012

dx.doi.org/10.1021/jp302907e | *J. Phys. Chem. B* 2012, 116, 10842−10855

synthesized in a variety of cells, predominantly in those which are implicated in the functioning of the organism immune system, like platelets,[3] neutrophils,[7] mast cells,[8] endothelial cells,[9−11] and lymphocytes.[12] Interestingly, PAF is not stored in the cell but is rapidly produced as a response to various external stimuli; thus, the increasing level of PAF is often connected with the inflammatory as well as other pathological conditions.[6]

It is known that the activity of PAF is connected with various inflammatory processes, among which edema formation,[13] endotoxic shock,[14] hyperpermeability in microvessels,[11,15] and angiogenesis[16] are important examples. Moreover, it was evidenced that proangiogenic and proinflammatory activities are implicated with tumor tissue growth and proliferation.[17−20] PAF is also involved in vascular barrier regulation, and since it accumulates in endothelium and subendothelial structures, the morphological and biochemical changes of endothelial cells occur.[15] The above-mentioned examples certainly do not exhaust the described subject and constitute only a fragment of broad activities demonstrated by PAF.[21−24]

Another interesting problem that should be discussed herein concerns the mechanism of PAF action. On one hand, it is widely known that the activity of this phospholipid is connected with its binding to the highly specific G-protein-coupled receptor (PAFR) localized particularly in membrane microdomains, like lipid rafts and caveolae.[25] In contrast, there is also a growing body of evidence that a number of important activities of PAF are manifested through the receptor independent mechanism,[8] and they are mainly attributed to the capability of PAF to incorporate into biomembrane structure. There are results of studies suggesting that the concentration-dependent intercalation of PAF into membrane leads to significant changes of its organization, properties, and function.[8,26−28] It was found that exogenous PAF can easily be incorporated into the outer membrane leaflet of erythrocytes, which leads to the alteration of cell shape and to the phosphatidylserine exposure.[29] In another study, Schneider and co-workers proved that, in the membrane of erythrocytes, the reorientation process ("flip-flop") of PAF molecules is possible from the outer to the inner layer.[30] PAF intercalation into red blood cell membrane was also reported by Chen, but the exact role of this phospholipid has not been described yet.[7] In the literature, there are also results suggesting that PAF, in a dose-dependent manner, causes lytic effects on the plasma membrane, leading to cell necrosis.[31] It is also worth mentioning that exogenous PAF cannot be efficiently decomposed by PAF acetylhydrolase;[32] therefore, the incorporation of this phospholipid into a membrane environment leads to different effects than those observed in the case of the endogenously synthesized PAF.

Unfortunately, studies concerning this issue are scarce; thus, it is not possible to draw any fundamental conclusions regarding the influence of PAF on the properties of cellular membranes. Moreover, most of the literature presents almost exclusively the results of studies carried out on the cell cultures, whereas there is lack of contributions focused on the simplified (model) systems, which are known to be very efficient in studies on molecular activities of lipids in membranes.[33,34] The studies performed in the membrane-mimicking systems open possibilities to characterize the interactions between lipid components at the molecular level. To the best of our knowledge, there is no evidence concerning the interactions between PAF and the main lipid components of natural membrane. This issue is of great importance in the perspective of potential applications of this highly active compound in pharmacology. Moreover, as mentioned above, the activity of PAF is related to its direct intercalation into cell membrane but so far the mechanism of this action has not been elucidated. In order to clarify this issue, we have planned and performed systematic experiments focused on the characterization of PAF behavior in membrane-mimicking environment. Our studies concern the representative of a double-chained choline-type phospholipid: 1,2-dipalmitoyl-*sn*-glycero-3-phosphocholine (DPPC) as well as the mammalian steroid occurring in membrane: cholesterol (Chol). Both compounds are widely distributed in the outer layer of biomembranes and are important structural components of lipid rafts, which is of great importance, bearing in mind that the concentration of PAF in natural membrane may be elevated in such microdomains. Moreover, in the case of exogenous incorporation of bioactive lipid into the cell membrane, the outer leaflet and in particular its lipid components should be considered as a primary target for PAF action. The influence of PAF on the model membrane ought to be tested in a broad range of mole fractions, since the concentration of PAF depends significantly on the origin of this phospholipid. Namely, according to the results published by other authors, PAF is synthesized in the membranes of stimulated cells, but normally it is not stored there.[6] Such a mechanism implies that the concentration of PAF in biomembranes is relatively low. On the other hand, it is possible to incorporate this ether phospholipid exogenously; thus, its concentration is directly connected with the administered doses and could be thus certainly larger than in the previous case. Plenty of studies underlined that PAF activity is strongly related to its concentration (dose-dependent mechanisms);[9,35,36] therefore, in our studies, we tested PAF activities in a wide range of concentrations (molar fractions) in model systems.

Having regard to the above, in the present study, we apply Langmuir monolayers as an excellent platform enabling the studies of interactions between lipids in a membrane-mimicking environment. A great advantage of such a methodology is the possibility to easily adjust and precisely control both the experimental conditions (surface pressure, temperature, etc.) as well as model membranes' compositions.

The investigated systems, namely, PAF/Chol and PAF/DPPC, were characterized with the measurements of surface pressure vs mean molecular area ($\pi-A$) isotherms in a broad range of mole fractions. The surface textures of the investigated films were visualized *in situ* with the application of μm-resolution Brewster angle microscopy (BAM). Finally, the interactions of lipids in binary monolayers were characterized at the molecular level by the grazing angle X-ray diffraction technique (GIXD). Combining the traditional Langmuir technique with modern physicochemical methods enables one to obtain broad knowledge on the interactions in both investigated systems: PAF/Chol and PAF/DPPC.

EXPERIMENTAL SECTION

Materials. The investigated single-chained phospholipid, C_{18}PAF (1-*O*-octadecyl-2-acetyl-*sn*-glycero-3-phosphocholine), of the highest purity available in stock (99%) was purchased from Bachem AG Switzerland and used without further purification. Cholesterol, Sigma grade (≥99%), and DPPC (1,2-dipalmitoyl-*sn*-glycero-3-phosphocholine), ≥99% (TLC), were purchased from Sigma-Aldrich. Spreading solutions of the lipids of the concentration close to 0.2 mg/mL were prepared

in chloroform/methanol 9/1 (v/v) mixture. Mixed solutions of the declared compositions were prepared from the respective stock solutions and deposited onto water subphase with the Hamilton microsyringe precise to 1 μL. Chloroform of spectroscopic purity (99.9% stabilized by ethanol) as well as methanol (99%) were provided by Sigma-Aldrich. In all experiments, the Langmuir trough was filled with ultrapure water of the resistivity ≥18.2 MΩ·cm^{-1} obtained from a Milli-Q system.

Methods. *Langmuir Experiments.* In routine experiments, π–A isotherms were registered with the NIMA (Coventry, U.K.) Langmuir trough of a total area of 300 cm^2 with a single movable barrier, placed on an antivibration table. The surface pressure was measured with an accuracy of 0.1 mN/m using a Wilhelmy balance equipped with a surface pressure sensor made of filter paper (ashless Whatman). In each experiment, the monolayer was left to equilibrate for at least 5 min before the monolayer compression was initiated with a barrier speed of 20 cm^2·min^{-1}, which corresponds to ca. 12 Å^2·molecule^{-1}·min^{-1}. The constant temperature during experiments (20 °C) was controlled thermostatically with the circulating water system.

BAM Visualization. The investigated monolayers were visualized with an ultraBAM apparatus (Accurion GmbH, Göttingen, Germany). The light source working in the microscope was a 50 mW laser emitting p-polarized light of 658 nm wavelength direct to the air/water interface at the Brewster angle (53.2°). The lateral resolution of the BAM image was 2 μm. The microscope was installed over a KSV (Helsinki, Finland) double-barrier Langmuir trough, model 2000 of a total area of ∼700 cm^2. The quantitative analysis of BAM images was performed with freely available ImageJ software.

GIXD Measurements. GIXD experiments were performed with the liquid surface diffractometer at the BW1 beamline in HASYLAB, DESY synchrotron center (Hamburg, Germany). The incidence X-ray wavelength of λ =1.303 Å was obtained by the reflection from a beryllium (200) monochromator crystal. In the Langmuir monolayer experiment, a single barrier trough of a total area of ca. 600 cm^2 (R&K, Potsdam, Germany) placed in a gastight container mounted on the goniometer of the diffractometer was used. In each experiment, after spreading the lipid solution on the water surface, the container cover was sealed and the canister was flushed with helium in order to reduce the oxygen level. The purpose of this procedure is to minimize the beam damage during reflectivity scans and reduce the scattering background. After at least 40 min, a monolayer was compressed to the target surface pressure (30 mN/m), which was held constant during the entire experiment. The construction of the BW1 beamline was described comprehensively in several previous articles;[37−40] therefore, we focus here only on the foundations of the GIXD technique.

The application of the GIXD technique allows one to obtain high resolution information regarding the in-plane organization of a Langmuir film in the Å scale. Diffraction of X-rays in the technique is possible only if the film-forming molecules are periodically organized at the interface. If the incidence X-ray radiation is scattered, its intensity can be measured by position sensitive detector (PSD). The obtained intensity can then be represented as a function of horizontal scattering vector (Q_{xy}) and the scattering vector component along the monolayer normal (Q_z), that is, as Bragg peak(s) and Bragg rod(s), respectively.

The scattered intensity is measured by scanning over a range of horizontal scattering vectors Q_{xy}, defined as

$$Q_{xy} \sim \frac{4\pi}{\lambda} \sin \theta_{xy} \tag{1}$$

where $2\theta_{xy}$ is the angle between the incident and diffracted beams projected onto the horizontal plane. Bragg peaks are resolved in the Q_{xy} direction, by integrating the scattered intensity over the Q_z. On the other hand, the Bragg rod profiles are resolved in the Q_z direction:

$$Q_z = \frac{2\pi}{\lambda} \sin \alpha_f \tag{2}$$

where α_f is the exit angle of the X-ray beam. Bragg rods are obtained by integrating the scattered intensity over Q_{xy} corresponding to the Bragg peaks.

Combination of the results obtained from the in-plane and out-of-plane measurements enables one to describe cell parameters as well as the arrangement of X-ray scattering moieties in the 2D crystalline lattice. On the other hand, lack of a signal in GIXD experiment is also important information, since it indicates that film-forming molecules are poorly organized in the monolayer plane and consequently do not participate in the formation of a 2D ordered phase.

Analysis of the π–A Isotherms. In order to gain fundamental information regarding the monolayer state, the traditional approach proposed by Riedel and Davies was applied.[41] According to the definition, the compression modulus, expressed as $C_s^{-1} = -A(d\pi/dA)$, was calculated from the π–A isotherms and then the dependencies of C_s^{-1} versus π were presented graphically.

The miscibility of the investigated lipids in mixed Langmuir monolayers as well as the interactions between components were analyzed quantitatively on the basis of the calculated values of the excess free energy of mixing (ΔG^{Exc}), defined as $\Delta G^{Exc} = N_A \int_0^{\pi} A_{12} - (A_1X_1 + A_2X_2)\, d\pi$, where A_{12} is the mean molecular area for a given composition of a binary film at a given surface pressure, A_1 and A_2 are the mean molecular areas for pure monolayers of components 1 and 2, respectively, taken at the same surface pressure, while X_1 and X_2 indicate molar fractions of the components in the mixture and N_A is Avogadro's number.[42]

The negative values of the excess free energy of mixing calculated for a given binary system indicate that the interactions between both components are more attractive (or less repulsive), as compared to the pure films of respective components. Furthermore, the negative values of ΔG^{Exc} can be treated as a factor indicating that both components are mutually miscible in a binary film. In contrast, the positive values of the excess free energy of mixing may suggest that interactions in mixed film are thermodynamically unfavorable, which may lead to the phase separation.

Parameters Calculated from the 2D Diffraction Pattern. The representation of the measured intensities as a function of Q_{xy}, Bragg peak(s), and Q_z, Bragg rod(s), opens a possibility to acquire a number of important parameters defining the 2D crystal lattice. Lattice parameters a and b can be correlated with the position of the Bragg peaks' maxima according to the most general relation:[43]

$$d = 2\pi/Q_{xy} = [h^2/a^2 + k^2/b^2 - 2(hk/ab)\cos\gamma]^{-1/2} \sin(\gamma) \tag{3}$$

where d is the lattice repeat distance in the 2D lattice, h and k are the Miller indices, and γ is the angle between lattice vectors of the given unit cell. For the hexagonal unit cell, $\gamma = 120°$, for rectangular $\gamma = 90°$, whereas for the oblique cell, the angle is $90° < \gamma < 120°$.

From these parameters, the area of the unit cell can be calculated according to the simple formula

$$A = ab \sin(\gamma) \tag{4}$$

It is also possible to estimate the range of the crystallinity in a monolayer from the Scherrer formula:

$$L_{xy} = 0.9\frac{2\pi}{\mathrm{fwhm}_{Q_{xy}}} \tag{5}$$

where $\mathrm{fwhm}_{Q_{xy}}$ is the full width at half-maximum of the Bragg peak.

Another important parameter is the value of the molecular tilt angle (τ), which describes the deviation from the upright orientation of the film-forming molecules:[44]

$$Q_{z,hk} = Q_{xy,hk} \tan(\tau) \cos\psi \tag{6}$$

where ψ is the angle between the tilt direction and the Q_{xy} vector.

Additionally, from the fwhm of the Bragg rod, according to the Scherrer formula, the thickness of the fraction of monolayer that coherently scatters X-ray radiation can be calculated:

$$L_z = 0.9\frac{2\pi}{\mathrm{fwhm}_{Q_z}} \tag{7}$$

The above formula similarly to eq 3 describes the order in the monolayer but in contrast to the former, along the direction perpendicular to the air/water interface. In the case of phospholipids, the L_z value provides information regarding the length of the hydrophobic moiety coherently scattering X-rays.

RESULTS AND DISCUSSION

We would like to begin the presentation and discussion of the experimental results with the data collected with the Langmuir technique. In Figure 1, the π–A isotherms registered for binary Langmuir films composed of PAF and cholesterol are shown.

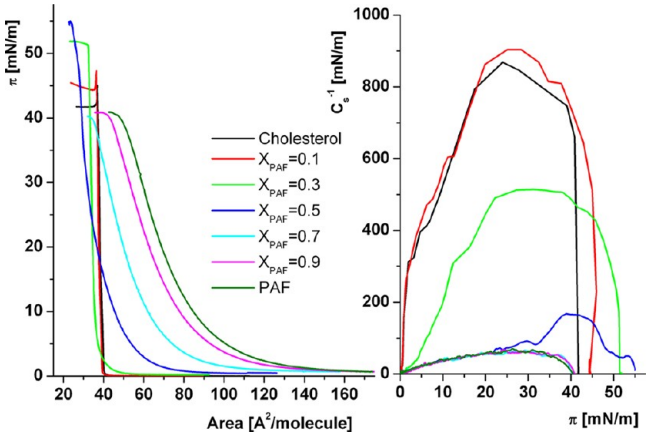

Figure 1. π–A isotherms registered for the PAF/cholesterol mixed monolayers together with the compressibility vs surface pressure dependencies.

The π–A isotherm for a monolayer of cholesterol is well documented in the literature, and our results are in a good agreement with these data.[45−47] In brief, it can be seen that the surface pressure starts to rise at a mean molecular area of 40 Å^2, while the collapse of monolayer occurs at ca. 37 Å^2/molecule, which corresponds to a surface pressure of 42 mN/m. The obtained isotherm exhibits the condensed nature of the cholesterol monolayer, which additionally finds its corroboration in the calculated values of compression modulus, the maximum of which reaches a value of ca. 880 mN/m. Such a high value is characteristic for the solid state of a monolayer, in which closely packed molecules are oriented perpendicular to the air/water interface. On the other hand, the π–A isotherm obtained for the monolayer of PAF has completely different characteristics. The surface pressure rises gradually from large molecular areas of ∼150 to 48 Å^2/molecule, where the collapse of monolayer starts to proceed. The course of the compression isotherm of PAF monolayer discloses its expanded (liquid-like) state, which was also confirmed on the basis of the values of C_s^{-1} vs π dependency. For more details concerning PAF film, please see our recent paper.[48] As far as the isotherms of mixed monolayers are concerned, it can be seen that the values of the surface pressures corresponding to the monolayers' collapses change systematically with the composition, which is a good prognostic for mutual miscibility of both components. Interestingly, the course of the isotherms registered for monolayers of $X_{PAF} = 0.1$ and 0.9 are very similar to those obtained for individual one-component films. This is also reflected in the compressibility plots, and it can be concluded that, in these cases, monolayers' states are similar to the pure monolayers of the dominating component. On the other hand, the most significant changes regarding the characteristics of mixed monolayers were found for $X_{PAF} = 0.3$ and 0.5; namely, at a first glance, one can see that the isotherms for these monolayers differ profoundly from those registered for one-component monolayers as well as for other mixed films. The analysis of C_s^{-1} vs π dependencies reveals that in comparison to pure cholesterol film, in the case of monolayers of $X_{PAF} = 0.3$ and 0.5, film condensation decreases significantly. Consequently, further increasing of PAF amount in mixed monolayers ($X_{PAF} = 0.7$ and 0.9) results in very low values of compression modulus, comparable to the values calculated for pure PAF monolayer.

The thermodynamic analysis of the interactions in mixed PAF/Chol films was carried out on the basis of the calculated values of the excess free energy of mixing (ΔG^{Exc}) plotted as a function of monolayer composition. The results are presented in Figure 2.

The ΔG^{Exc} values for the aforementioned system are strongly negative in the whole range of mole fractions. Such results indicate that the interactions between both components of the binary monolayer are more attractive as compared to those existing in pure films of respective components. The undertaken analysis of the excess free energy of mixing discloses that the miscibility of both components is a thermodynamically favorable process. Also, it can be concluded that, for the $X_{PAF} = 0.3$ and 0.5, where the lowest values of ΔG^{Exc} were found, mixed PAF/Chol monolayers are most stable.

Let us now discus BAM images taken for the binary monolayer composed of PAF and cholesterol. Generally, our considerations are focused on the results obtained for a monolayer compressed to a surface pressure of 30 mN/m, since at this value of surface pressure the properties of model system

dx.doi.org/10.1021/jp302907e | J. Phys. Chem. B 2012, 116, 10842−10855

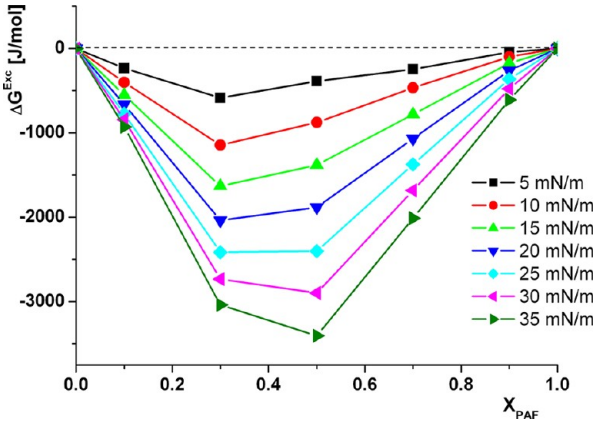

Figure 2. The excess free energy of mixing (ΔG^{Exc}) calculated for the mixed monolayer of PAF/cholesterol as a function of PAF content. The calculated points were connected by continuous lines in order to improve the clarity of presentation.

can be referred to the state and molecular organization in natural biomembranes.[49] However, for presentation of BAM images, we have chosen both photos taken at a surface pressure of 10 mN/m as well as 30 mN/m, as they represent a large diversity of textures and therefore provide excellent insight into the surface textures of the investigated monolayers.

At the beginning, it is worth mentioning that, in the case of pure cholesterol film, the recorded images confirm that the monolayer is homogeneous in a wide range of surface pressures (see the Supporting Information, Figure S1). Characteristic foam-like structures are visible only at π = 0 mN/m, for large mean molecular areas. After the monolayer compression has been initialized, the image becomes homogeneous until the collapse, which manifests in the appearance of initially small shining structures that subsequently grow into larger 3D crystallites. Similarly, the image recorded for the PAF monolayer is uniform almost during the entire compression; namely, bright spots are visible only for the surface pressure close to the monolayer collapse. On the other hand, images registered for the mixed PAF/Chol monolayers are far more interesting. As mentioned above, in the case of pure cholesterol film, at π = 10 mN/m, the observed image reveals monolayer homogeneity; however, even if a small amount of PAF was added (X_{PAF} = 0.1), the monolayer structure changes significantly (Figure 3). The grayscale of the image is no longer uniform and—as can be seen—large bright domains of condensed phase coexist with darker regions of expanded phase. Moreover, it can be noticed that numerous small domains separate from the large homogeneous phase. With increasing amount of PAF in monolayer, the bright condensed phase becomes intersected by thin regions of lower surface density (X_{PAF} = 0.3). Further division of the condensed monolayer can be clearly visible in the next three images

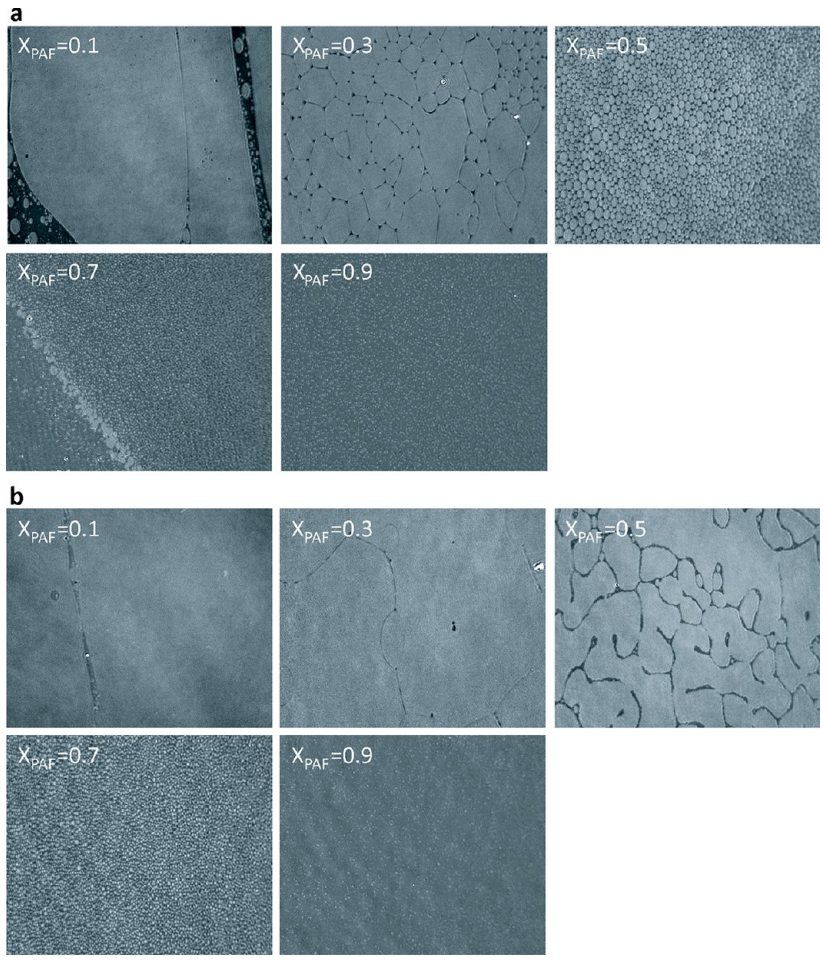

Figure 3. BAM images registered for a mixed monolayer of PAF/cholesterol at 10 mN/m (a) and 30 mN/m (b).

dx.doi.org/10.1021/jp302907e | J. Phys. Chem. B 2012, 116, 10842−10855

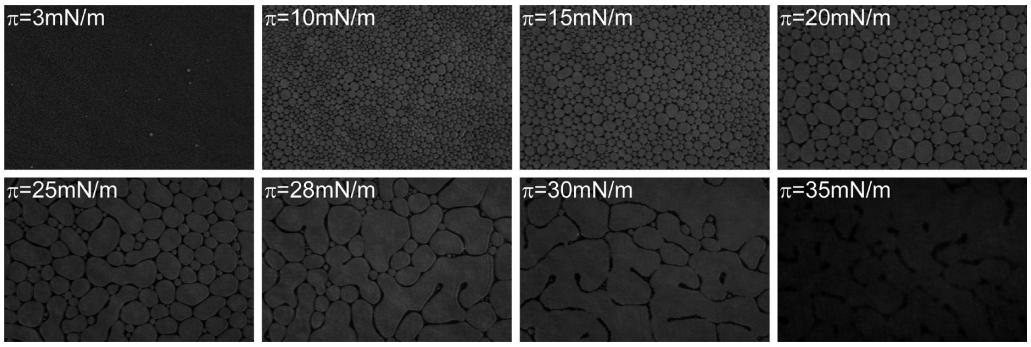

Figure 4. BAM images registered during compression of the PAF/Chol 0.5/0.5 monolayer.

registered for the content of PAF equal to 0.5, 0.7, and 0.9. Finally, in the last two cases, the condensed domains turn into small spots of a weak contrast, hardly visible in the photos. The evolution of BAM images upon PAF addition was also found in the case of a biologically relevant surface pressure of 30 mN/m. The above-mentioned photos are shown in Figure 3b. It can be seen that, for monolayers of X_{PAF} = 0.1 and 0.3, the registered images show almost homogeneous. The situation changes for PAF/Chol 0.5/0.5; namely, the bright large structures of an irregular shape coexist at the interface with the dark elongated regions characteristic for the expanded phase. Finally, for the higher proportion of single-chained phospholipid (X_{PAF} = 0.7 and 0.9), the recorded images are similar to those observed in the case of a surface pressure of 10 mN/m. Such a presentation of the results provides information regarding monolayers' morphology changes depending on PAF molar fraction. However, in order to describe the evolution of the observed domains during monolayer compression, the additional data are needed. In Figure 4, BAM images registered for the equimolar mixture of PAF/Chol are presented.

BAM photos included in Figure 4 show the sequence of the domains' transformation depending on the surface pressure. Generally, it can be noticed that the size of the condensed domains increases upon film compression from the surface pressure of ca. 10 mN/m and finally, at $\pi \sim 30$ mN/m, islands of the condensed phase merge together into large irregular platforms. This phenomenon can be quantitatively described by comparing the estimated areas occupied by the condensed domains. Namely, for a surface pressure of 10, 15, and 20 mN/m, the maximal size of the observed domains falls within the range 355−390, 500−645, and 1000−2140 μm^2, respectively. Interestingly, at $\pi \sim 25$ mN/m, larger 2−4 domains' conglomerates, occupying a surface of ca. 4500−6850 μm^2, can be seen on the surface. With further compression to π = 28 mN/m, the condensed domains merge into larger structures of 8000−23400 μm^2. Interestingly, at a surface pressure of 30 mN/m, it is not possible to estimate the size of the largest domains because of the disappearance of sharp boundaries between them.

It can be concluded that the addition of the investigated single-chained phospholipid into a monolayer of cholesterol causes dramatic changes in its characteristics. It is not surprising, since it is well-known that both lipids of the binary mixture behave quite differently in their pure monolayers. Cholesterol, similarly to other sterols, forms a solid-type monolayer, and furthermore, it is evident, in particular on the basis of GIXD measurements, that cholesterol molecules are oriented perpendicularly to the air/water interface.[50−53] On the other hand, single-chained phospholipids, bearing in their structures a large choline headgroup, cannot organize themselves into highly ordered 2D crystalline domains. Instead of this, as it has been proved in our former paper,[48] PAF molecules form a disordered phase, in which molecules are strongly tilted from the surface normal, and, additionally, they are strongly immersed in the water subphase. The quantitative analysis performed for BAM images gathered in Figure 4 revealed that, for an equimolar ratio of PAF/Chol, surface morphology changes drastically as compared to films containing a lower amount of PAF, and even at a relatively high surface pressure of 30 mN/m, the mixed monolayer is not homogeneous. This is an important finding, since it indicates that, at this very proportion of both lipids, the μm-scale properties of model membrane change significantly. Moreover, in the further section devoted to the discussion of the GIXD results, we will show that the binary monolayer of PAF/Chol 0.5/0.5 compressed to a surface pressure of 30 mN/m is not ordered periodically.

Let us proceed to the system PAF/DPPC. In Figure 5, the π−A isotherms together with the compressibility modulus vs surface pressure dependencies collected for this system are presented.

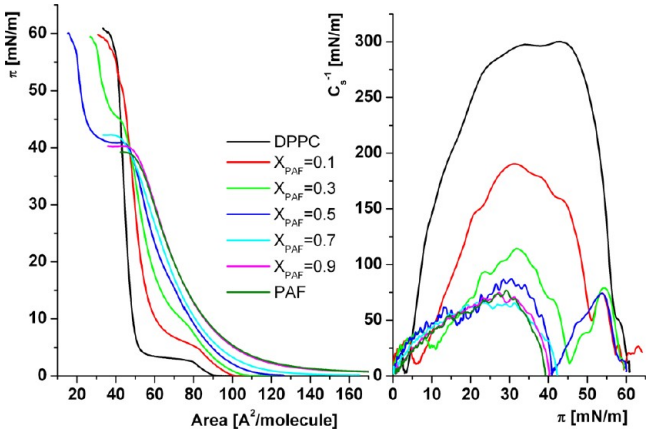

Figure 5. π−A isotherms registered for the PAF/DPPC mixed monolayers together with the compressibility vs surface pressure dependency.

The results obtained for DPPC monolayer are in agreement with those presented previously by us[47,50] as well as by other authors.[54] The characteristic feature of the discussed curve is the presence of a phase transition between the liquid expanded and condensed phase,[55] which reflects in the isotherm as a plateau region, spanning at the surface pressure of ca. 4 mN/m.

dx.doi.org/10.1021/jp302907e | J. Phys. Chem. B 2012, 116, 10842−10855

This plateau appears also in the isotherms recorded for mixed films of X_{PAF} = 0.1, 0.3, as well as 0.5; however, in the latter case, it should be rather referred to as a kink. For a higher proportion of PAF in the mixed monolayer, phase transition disappears and the curves rise monotonically until the film collapse. As far as the collapse of the monolayer is concerned, it is evident that, for mixtures of X_{PAF} = 0.1, 0.3, and 0.5, the surface pressure increases even after inflection (first collapse) at high surface pressure (>40 mN/m) is visible in the course of the isotherm. This may suggest the existence of phase separation above the surface pressure corresponding to the collapse of a particular component in a mixed film, and will be discussed thoroughly later on, based on BAM images. In order to get a deeper insight into miscibility in PAF/DPPC film, the surface pressure values corresponding to both phase transition and monolayers' collapses have been presented in Figure 6 as a function of film composition.

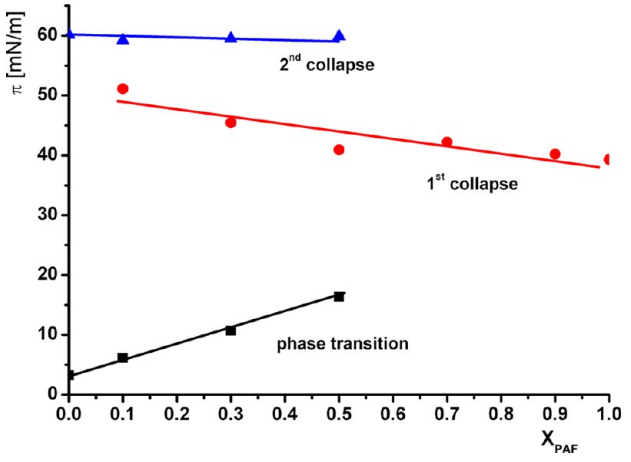

Figure 6. Collapses and phase transition pressures for the mixed PAF/DPPC monolayers.

It can be seen that the values of the surface pressures characteristic for both phase transition as well as the first collapse change with film composition, suggesting miscibility of the components in binary monolayers up to the first collapse. On the other hand, above this value, a phase separation occurs and the second collapse observed at the value of surface pressure characteristic for the phase rich in DPPC does not depend on the molar fraction of PAF in the range of $X_{PAF} \leq 0.5$.

It is worth mentioning that, similarly to the above-mentioned mixtures of PAF/Chol, the addition of PAF to the monolayer of DPPC gives rise to the decrease of the monolayer condensation, which can be easily confirmed by the analysis of the maximum values of the compressibility modulus. Starting from X_{PAF} = 0.5, the state of monolayers can be classified as liquid expanded, in which the film-forming molecules are disordered at the air/water interface.

In Figure 7, the calculated values of the excess free energy of mixing were plotted as a function of monolayer composition.

On the basis of thermodynamic considerations, we are able to draw conclusions regarding the mutual miscibility of PAF and DPPC in their mixed films. Namely, the positive values of the excess free energy of mixing (ΔG^{Exc}) calculated for the investigated system suggest that the mixing of both compounds is a thermodynamically unfavorable process. Moreover, the obtained results prove that the interactions in a binary

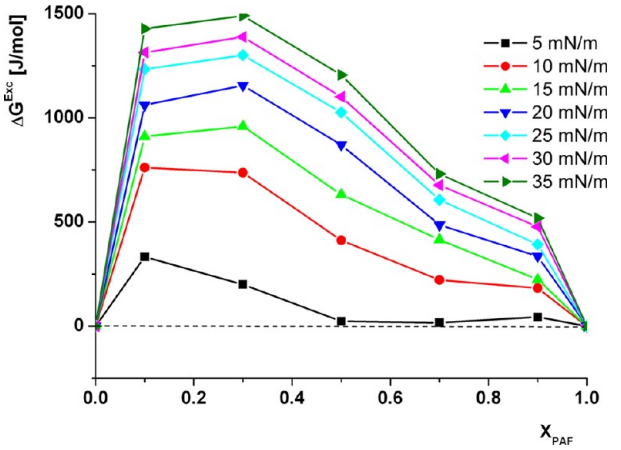

Figure 7. The excess free energy of mixing (ΔG^{Exc}) calculated for the mixed monolayer of PAF/DPPC as a function of PAF content. The calculated points were connected by continuous lines in order to improve the clarity of presentation.

monolayer of PAF/DPPC are more repulsive (or less attractive) as compared with those existing in pure monolayers of respective phospholipids.

In a further experiment, the investigated binary monolayers composed of PAF and DPPC were visualized *in situ* with Brewster angle microscopy and the recorded images were gathered in Figure 8.

In Figure 8a, images were acquired for a monolayer of DPPC as well as PAF/DPPC compressed to a surface pressure of 10 mN/m are presented. For pure DPPC film, such a value of π corresponds to the region in the isotherm just above the plateau; therefore, in the image, closely packed condensed domains of ca. 175−345 μm^2 are visible. These domains are characteristic for a monolayer of DPPC and appear in the liquid expanded and liquid condensed phase coexistence region.[56] It is evident that, with increasing PAF content in the binary film, visualized at the same surface pressure (10 mN/m), the condensed domains of a snowflake shape become smaller (25−170 μm^2) and are more dispersed in the expanded phase (dark regions in the photos). For the monolayer of X_{PAF} =0.3, only small bright spots of an average size of ca. 39 μm^2 are visible which finally vanish with further addition of the single-chained phospholipid into the mixed monolayer (photos not shown). In the case of pure DPPC film compressed to a surface pressure of 30 mN/m, the BAM image presented in Figure 8b looks homogenous; however, with the increasing amount of PAF, separated condensed domains appear at the surface. In the case of PAF/DPPC 0.1/0.9 and 0.3/0.7 monolayers, these domains occupy areas of 125−290 μm^2 and 215−1040 μm^2, respectively. For larger proportions of PAF, namely, X_{PAF} = 0.5 and 0.7, they become smaller (55−325 and ∼33 μm^2, respectively), whereas distances between them enlarge. Finally, for the system composed of PAF/Chol 0.9/0.1, structures of a condensed state are no longer visible on the surface (image not shown). The analysis of BAM images provides interesting conclusions regarding the behavior of the studied single-chained ether phospholipid in model membrane containing DPPC. One can find that in the case of mixed PAF/DPPC monolayers, to reach the comparable size and shape of condensed domains, the film with a larger amount of PAF needs to be compressed to significantly higher surface pressure. For example, structures observed for a monolayer of DPPC at a surface pressure of 10

dx.doi.org/10.1021/jp302907e | J. Phys. Chem. B 2012, 116, 10842−10855

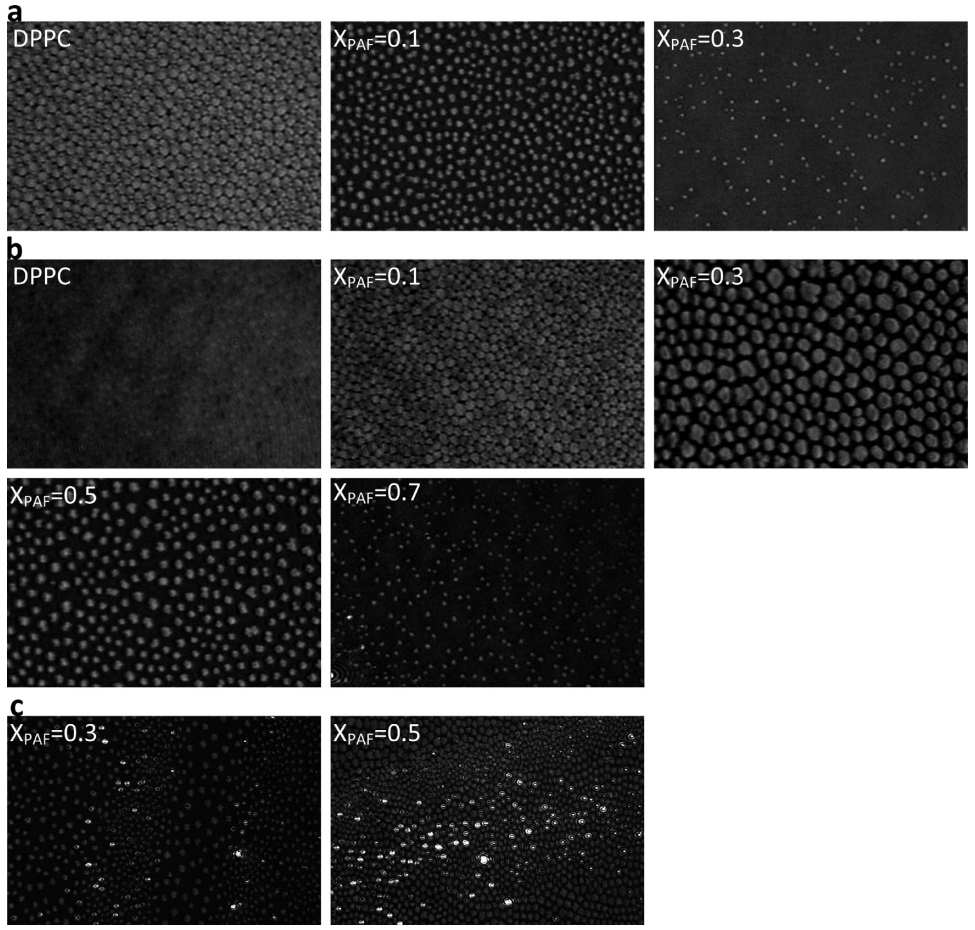

Figure 8. BAM images registered for a mixed monolayer of PAF/DPPC at 10 mN/m (a), 30 mN/m (b), and 50 mN/m (c).

mN/m are very similar to those recorded for PAF/DPPC 0.1/0.9 at π = 30 mN/m, whereas small domains in PAF/DPPC 0.3/0.7 (π = 10 mN/m) resemble those in PAF/DPPC 0.7/0.3 mixture at π = 30 mN/m. It means that, in order to obtain a higher surface density for a model membrane rich in poorly organized molecules (e.g., PAF), the applied force (surface pressure) has to be notably higher.

It is worth mentioning that the miscibility between film components cannot be excluded, although thermodynamic considerations reveal unfavorable interactions between PAF and DPPC and BAM images show inhomogeneity of monolayers even at higher surface pressure (30 mN/m). This situation changes when the surface pressure exceeds the value corresponding to the first collapse, which is visible in the course of the isotherms for a monolayer of X_{PAF} = 0.3 and 0.5. The images of the mentioned films are presented in Figure 8c. It can be seen that small domains of condensed phase coexist with small shining spots, which are typical for the formation of 3D crystallites at the interface. In this case, such phase separation is caused by the fact that one component of a binary mixture (PAF) has a significantly lower collapse pressure than the other one (DPPC). Namely, the investigated pure monolayers of PAF and DPPC collapse at ca. 40 and 60 mN/m, respectively; thus, at π = 50 mN/m, molecules of PAF can be expelled from the binary film, forming a 3D phase.

The results discussed so far provide conclusions regarding the basic characteristics of the investigated binary monolayers. Parameters deduced from the π–A isotherms provide information about the monolayers' state; it was found out that the addition of PAF into both Chol and DPPC film causes significant changes of monolayer compressibility. On the other hand, it was evidenced that the interactions in PAF/Chol and PAF/DPPC films are quite different. In the former case, the interactions are more attractive than in pure monolayers of the respective compounds, while for the latter system they are thermodynamically unfavorable. Such an analysis may lead to the conclusion regarding the miscibility in the investigated systems; namely, PAF and Chol mix in the whole range of molar fractions, while in the system composed of PAF and DPPC a phase separation (especially at higher surface pressure) may occur. It should be, however, emphasized that these findings concern only global properties, which are averaged for the monolayer treated as a macroscopic object. Such an overall approach does not explain microscopic and especially molecular properties; therefore, the application of the complementary techniques is of great importance. Brewster angle microscopy enables us to visualize the surface in the micrometer scale, but to go deeper into the organization of a monolayer, we need to apply a more powerful technique. The application of synchrotron X-ray radiation with an initial wavelength of 1.303 Å makes it possible to obtain Angström resolution; therefore, to investigate monolayers at the molecular level, we have applied the GIXD technique. All of the presented GIXD scans were carried out for the monolayers compressed to 30 mN/m, since it is known that such conditions in model systems can be very well correlated with the properties of natural membranes. Systematic characteristics have been performed in the broad range of molar fractions; however, in the case of

dx.doi.org/10.1021/jp302907e | J. Phys. Chem. B 2012, 116, 10842–10855

PAF/Chol binary films, the diffraction signal was acquired only for the molar fraction of X_{PAF} = 0.1 and 0.3. For larger amounts of PAF, a diffraction pattern was not obtained, which is also valuable information, since it indicates that these monolayers are not periodically ordered. This is not surprising, as PAF forms a monolayer of an expanded state, in which molecules are disordered at the interface. Hence, with the increase of PAF content in the mixed monolayer, its condensation decreases rapidly, which was proved in the preliminary studies described above. It should also be stressed that, in the case of the PAF/Chol system investigated at 30 mN/m, there is a direct connection between monolayers' morphology observed with BAM and Å-scale molecular organization described by GIXD. Namely, diffraction peaks were registered only for the homogeneous monolayers (PAF/Chol 0.1/0.9 and 0.3/0.7), while in the case of PAF/Chol 0.5/0.5 the signal was not obtained.

In Figure 9, the diffracted intensities as a function of in-plane scattering vector Q_{xy} (Bragg peaks) for a monolayer of cholesterol and mixed systems of PAF/Chol were gathered.

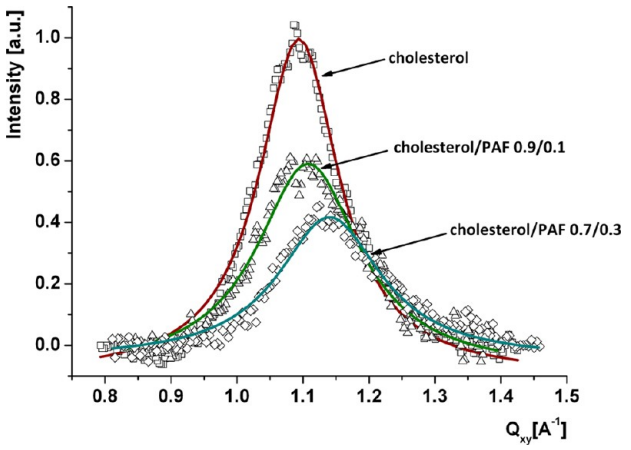

Figure 9. Diffracted intensity vs in-plane scattering vector Q_{xy} (Bragg peak) registered for a monolayer of cholesterol and a binary system of PAF/cholesterol.

On the basis of the GIXD experiments carried out for a monolayer of cholesterol as well as for PAF/cholesterol 0.1/0.9 and 0.3/0.7, one can find that the only one symmetrical diffraction signal occurs. The maximum intensity for these Bragg peaks is localized in the horizon, i.e., at Q_z = 0 Å^{-1}. The corresponding Bragg rods were presented in Figure S2 in the Supporting Information.

Such a diffraction pattern is characteristic for a monolayer, in which untilted molecules are closely packed at the interface. The organization of the cholesterol 2D lattice in our study was approximated to hexagonal; however, it was also reported in the literature that alternatively, according to molecular modeling, a cholesterol monolayer structure of trigonal symmetry $p3$ can be assigned.[51]

Comparing the intensity of the registered Bragg peaks, it is evident that, in the case of mixed monolayers, highly ordered hexagonal domains are formed from the smaller fractions of film-forming molecules. Namely, the ratio of the integrated Bragg peaks was estimated to be 1:0.4:0.1, which means that, with the increasing content of PAF, the number of molecules involved in formation of periodically arranged domains diminishes significantly. On the other hand, the registered Bragg peaks both for the monolayer of cholesterol and for PAF/Chol mixtures demonstrate comparable widths; therefore, the L_{xy} values are very similar. Consequently, the range of crystallinity in the investigated films is almost identical, which indicates that the presence of PAF in mixed hexagonal domains does not change their dimensions. This result is in agreement with BAM images registered for the investigated monolayers at 30 mN/m; namely, even at the μm scale, surface textures are very similar and do not change until the molar fraction of PAF in mixed film reaches 0.5.

The lattice parameters together with other structural factors calculated on the basis of GIXD data are compiled in Table 1.

As far as the lattice parameters for a monolayer of cholesterol and its mixtures with PAF are concerned, it is evident that, with increasing PAF amount in mixed monolayers, the 2D unit cell becomes smaller. It can be clearly seen from the comparison of the hexagonal unit cell areas calculated for the investigated monolayers. Such a result is connected to the fact that the

Table 1. Structural Parameters Calculated for Investigated Monolayers from GIXD Data

composition of monolayer	Bragg peak Q_{xy} (Å^{-1})	Bragg rod Q_z (Å^{-1})	lattice parameters (Å, Å, deg)	area (Å^2)	L_{xy} (Å)	tilt, τ (deg)	L_z (Å)
Chol	1.094 ± 0.001	0	$a = b$ = 6.628 ± 0.005	38.04 ± 0.04	38 ± 4	0	12.7 ± 0.1
			γ = 120				
PAF/Chol 0.1/0.9	1.108 ± 0.001	0	$a = b$ = 6.548 ± 0.006	37.13 ± 0.03	30 ± 5	0	10.1 ± 0.1
			γ = 120				
PAF/Chol 0.3/0.7	1.140 ± 0.001	0	$a = b$ = 6.361 ± 0.007	35.04 ± 0.03	30 ± 4	0	9.4 ± 0.2
			γ = 120				
DPPC	⟨−1, 1⟩ 1.467 ± 0.001	⟨−1, 1⟩ 0.099 ± 0.001	a = 4.990 ± 0.001	23.18 ± 0.04	$L_{\langle -1,1\rangle}$ 271 ± 6	26.8 ± 0.1	$L_{\langle -1,1\rangle}$ 19.6 ± 0.3
	⟨1, 0⟩ 1.393 ± 0.002	⟨1, 0⟩ 0.544 ± 0.007	b = 5.142 ± 0.001		$L_{\langle 1,0\rangle}$ 50 ± 5		$L_{\langle 1,0\rangle}$ 21 ± 2
	⟨0, 1⟩ 1.352 ± 0.001	⟨0, 1⟩ 0.618 ± 0.008	γ = 115.4 ± 0.1		$L_{\langle 0,1\rangle}$ 68 ± 4		$L_{\langle 0,1\rangle}$ 22 ± 2
PAF/DPPC 0.1/0.9	1.495 ± 0.001	0	$a = b$ = 4.851 ± 0.002	20.38 ± 0.02	152 ± 9	0	14.7 ± 0.7
			γ = 120				
PAF/DPPC 0.3/0.7	1.490 ± 0.001	0	$a = b$ = 4.867 ± 0.002	20.51 ± 0.03	124 ± 7	0	12.1 ± 0.3
			γ = 120				
PAF/DPPC 0.5/0.5	⟨0, 2⟩ 1.478 ± 0.001	⟨0, 2⟩ 0	a = 5.455 ± 0.005	46.36 ± 0.03	$L_{\langle 0,2\rangle}$ 202 ± 8	24.4 ± 0.2	$L_{\langle 0,2\rangle}$ 13.4 ± 0.4
	⟨−1, 1⟩ 1.368 ± 0.001	⟨−1, 1⟩ 0.65 ± 0.01	b = 8.498 ± 0.002		$L_{\langle -1,1\rangle}$ 43 ± 3		$L_{\langle -1,1\rangle}$ 18 ± 3
			γ = 90				

dx.doi.org/10.1021/jp302907e | J. Phys. Chem. B 2012, 116, 10842−10855

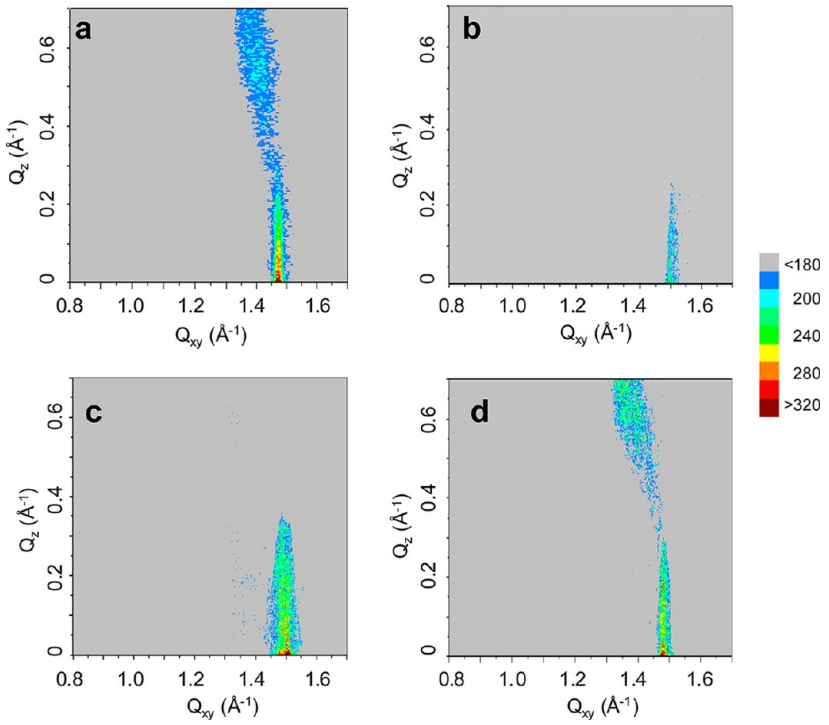

Figure 10. GIXD intensity maps, $I(Q_{xy}, Q_z)$, for a monolayer of DPPC (a), PAF/DPPC 0.1/0.9 (b), PAF/DPPC 0.3/0.7 (c), and PAF/DPPC 0.5/0.5 (d) compressed to a surface pressure of 30 mN/m.

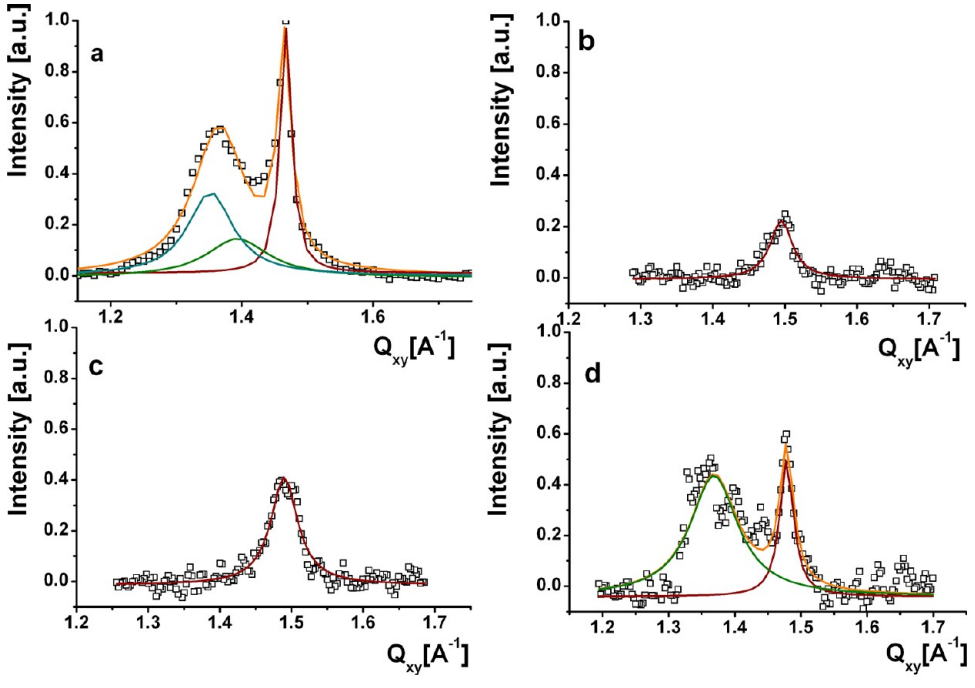

Figure 11. Diffracted intensity vs in-plane scattering vector Q_{xy} (Bragg peak) registered for a monolayer of DPPC (a), PAF/DPPC 0.1/0.9 (b), PAF/DPPC 0.3/0.7 (c), and PAF/DPPC 0.5/0.5 (d). The total and component Bragg peaks were fitted with the Lorentz function (continuous lines).

maxima of Bragg peaks shift toward higher values of Q_{xy} in the case of monolayers with larger proportions of PAF. Interestingly, the addition of PAF molecules to the monolayer of cholesterol does not lead to the change of the unit cell type; namely, in all three cases, only one diffraction signal at $Q_z = 0$ Å^{-1} was recognized. Such a finding means that the limited incorporation of molecules, which itself form a disordered strongly tilted monolayer into the well organized monolayer of cholesterol, does not ruin the highly ordered phase. It also means that the condensed mixed domains of PAF/Chol are formed at the interface until it is possible to retain the upright orientation of the molecules; otherwise (for the larger PAF amount), the monolayer completely loses its periodicity and the diffraction signal cannot be acquired.

dx.doi.org/10.1021/jp302907e | J. Phys. Chem. B 2012, 116, 10842−10855

Another interesting conclusion can be drawn from the comparison of the values of L_z parameter, which can be treated as the length of the coherently scattering part of molecules in film. For the pure monolayer of cholesterol, L_z is equal to 12.7 Å, which is in agreement with the previously published data.[50] The value of L_z becomes smaller when the content of PAF in mixed monolayer increases; thus, it indicates that PAF molecules, which are strongly immersed into the water subphase,[48] are involved in the formation of the highly ordered domains, and as a consequence of this, average thickness of the mixed monolayers decreases. The obtained results suggest that, in the case of natural membrane rich in cholesterol, such as lipid rafts or caveolae, the external incorporation of PAF does not disturb the organization and properties of cholesterol domains until the ratio of PAF:Chol reaches 1:2.

Let us now discuss the results obtained from the GIXD measurements for PAF/DPPC binary films. The intensity maps ($I(Q_{xy}, Q_z)$) for the above-mentioned system were presented in Figure 10. Similarly to the case of PAF/Chol mixed systems, all GIXD scans were performed for the monolayers compressed to 30 mN/m. It is also worth mentioning that, for the larger proportion of PAF in the mixed systems, i.e., for molar fractions of $X_{PAF} > 0.5$, the diffraction pattern was not acquired. This finding means that the molecular organization in monolayers is not periodical; therefore, the synchrotron radiation cannot be scattered by the randomly oriented molecules. Taking into account the quantitative analysis of BAM images obtained for monolayers of PAF/DPPC 0.5/0.5 and 0.7/0.3, the mentioned loss of periodicity is not surprising, since in the latter case the surface domains cover a significantly smaller area in the image and are even 10 times smaller than in the case of an equimolar monolayer of both lipids.

In the case of pure DPPC monolayer, the signal of the highest intensity denoted as $\langle -1, 1\rangle$ is localized close to the horizon, but at $Q_z > 0$, while in the region of Q_z spanning in the range of ca. 0.5−0.7 Å^{-1}, another peak(s) can be distinguished. Detailed analysis of the diffraction pattern leads to the conclusion that there are three distinct Bragg peaks with their maxima at Q_z = 0.099 Å^{-1} (1.467 Å^{-1}), Q_z = 0.544 Å^{-1}(1.393 Å^{-1}), and Q_z = 0.618 Å^{-1} (1.352 Å^{-1}). For details, see Figure 11a as well as Figures S3 and S4 in the Supporting Information. Such a distribution of scattered intensities ($Q_z^{\langle 0,1\rangle} \approx Q_z^{\langle -1,1\rangle} + Q_z^{\langle 1,0\rangle}$) is characteristic for the oblique 2D crystal structure, which was previously reported in the case of DPPC film.[57−61] From the registered signals, the main structural parameters were calculated and gathered in Table 1. Among them, the value of molecular tilt was calculated and equals 26.8°. This value is typical for the monolayer of double-chained phospholipids bearing a large choline headgroup, compressed to the surface pressure of ca. 30 mN/m.[58] The characteristic feature of the oblique unit cell is that film-forming molecules are tilted from the monolayer normal along the intermediate azimuth, that is, between the NN and NNN direction.

As far as the binary monolayers of PAF/DPPC are concerned, they will be discussed in the following order: first of all two mixtures with a PAF content of 0.1 and 0.3 and after that the equimolar film (X_{PAF} = 0.5).

For the mixed monolayer of PAF/DPPC 0.1/0.9 as well as PAF/DPPC 0.3/0.7, in the diffraction pattern, only one peak can be distinguished, which may lead to the conclusion that molecules of phospholipids are organized in the hexagonal lattice. There is no signal localized beyond the horizon; hence, molecules in the monolayer assume an upright orientation.

At first glance, this result seems to be quite strange, as it is well established that molecules of choline-type phospholipids demonstrate significant molecular tilt from the direction perpendicular to the air/water interface. Such a behavior was also proved above in the case of pure DPPC film. Moreover, assuming that the monolayer of PAF is in a liquid expanded state which was confirmed based on the π−A isotherms and also from the GIXD results (no diffraction), it is difficult to expect a well ordered hexagonal phase formed by the mixture of PAF and DPPC. On the other hand, the obtained Bragg peaks for both PAF/DPPC mixtures are comparatively weak, which indicates that only a small portion of film-forming molecules is involved in the formation of the 2D crystalline phase. Namely, the ratio of the integrated Bragg peak intensity was calculated to be 1:0.11:0.25:0.72, for a monolayer of DPPC and other three films with increasing molar fraction of PAF, respectively. The obtained trend indicates that the most disturbing effect (the lowest intensity of diffraction signal) is connected with the smallest amount of PAF in the mixed monolayer, i.e., X_{PAF} = 0.1, while for the higher PAF content (X_{PAF} = 0.3 and 0.5), the intensity of the signals increases, which means that a larger portion of molecules are involved in formation of periodically ordered domains. Additionally, the observed range of crystallinity (L_{xy} values) in the case of PAF/DPPC 0.1/0.9 and PAF/DPPC 0.3/0.7 monolayers is obviously smaller as compared to the pure DPPC film, which indicates that condensed lipid domains shrink. It should also be noticed that the coherence length in the direction perpendicular to the air/water interface (L_z) decreases in the case of above-mentioned mixed films. This fact is an additional confirmation for the concept of highly ordered mixed domains composed of PAF and DPPC in the molar proportion of 0.1/0.9 and 0.3/0.7. Similarly to the case of PAF mixtures with cholesterol, the estimated average monolayer thickness reduces as a result of incorporation of strongly immersed in subphase PAF molecules into condensed domains.

The above interpretation is in agreement with the data obtained with the GIXD technique; however, intuitively, these results may be rather surprising. Namely, it can be expected that the incorporation of the fraction of molecules, which in one component monolayer are disordered at the interface (PAF), to the surface film of DPPC, which is known to form intermediate tilted phase, should rather lead to the deepening of molecular tilt and/or increasing of monolayer disorder. Moreover, both PAF and DPPC possess a large choline headgroup, which does not favor the highly ordered packing of molecules at the interface. Despite this, the experimental data reveal quite an opposite effect; therefore, molecular organization in the mentioned monolayers was approximated to hexagonal.

Alternatively, it could be assumed that the diffraction signals registered for a monolayer of X_{PAF} = 0.1 and 0.3 originate from small amounts of equimolar domains of PAF/DPPC. In this case, it should be, however, accepted that the fraction scattering X-ray radiation is very small; therefore, only the most intense signal localized at Q_z = 0 Å^{-1} can be seen in the diffraction pattern. Consequently, the lower intensity of the Bragg peak registered for a monolayer of X_{PAF} = 0.1 as compared to X_{PAF} = 0.3 can be attributed to the diminishing of the equimolar fraction in monolayer.

The most interesting case concerns the above-mentioned binary mixture composed of the equimolar proportion of both phospholipids. As can be seen in the $I(Q_{xy}, Q_z)$ plot presented

in Figure 10d, the diffractogram for this mixture does not resemble those obtained for the other molecular fractions of PAF, but instead, it looks similar to the intensity map of DPPC. The key difference is that the position of the most intense peak has its maximum at the horizon (Q_z = 0). The second Bragg peak denoted as ⟨−1, 1⟩ is localized at Q_z = 0.65 Å^{-1} with its maximum at Q_{xy} = 1.368 Å^{-1}. Such an intensity distribution is characteristic for the monolayer in which molecules are organized in the centered rectangular lattice with the molecular tilt turned toward the nearest neighbor (NN).[62]

At this point, a question arises: what is the exact composition of the crystalline domains that coherently scatter X-ray radiation in the case of monolayer composed of PAF/DPPC 0.5/0.5, and consequently, why is such a surface arrangement favorable? First of all, it can be seen that the appearance of the additional diffraction signal localized beyond the horizon implies that the 2D crystalline lattice changed and that the molecules became tilted from the surface normal.

Additionally, the obtained diffraction signal is very intense, which indicates that most of the film-forming molecules are arranged periodically within the monolayer. It is also characteristic that the thickness of the monolayer fraction involved in formation of the crystalline domains decreases in the case of the discussed mixed system. Bearing these arguments in mind, a different model of molecule arrangement in 2D crystals was proposed and presented schematically in Figure 12.

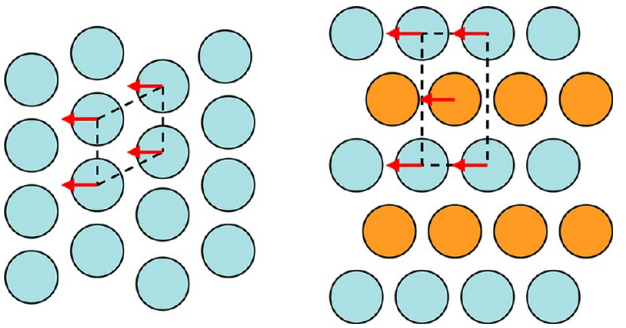

Figure 12. Schematic representation of the arrangement of phospholipid acyl chains; top view: DPPC (light blue circles) and PAF (orange circles). The contours of the unit cells were indicated with dashed lines (DPPC, oblique; PAF/DPPC 0.5/0.5, centered rectangular). Red arrows show the direction of the molecular tilt.

In the postulated model, molecules of PAF and DPPC form highly ordered mixed domains of the fixed stoichiometry. In the centered rectangular unit cell of the area of 46.36 Å^2, one molecule of PAF is localized in the center of a cell, while four acyl chains of DPPC are positioned in the corners of the rectangle. Thus, the unit cell contains two acyl chains, one from each molecule (PAF and DPPC). It should be however underlined that the stoichiometry suggested above for the unit cell does not correspond to the proportion of lipids in the mixed monolayer. On the other hand, the proposed molecular arrangement represents the most probable model in which PAF and DPPC molecules are organized in the rectangular centered unit cell. Within the monolayer, the domains of such ordering coexist with the regions of different molecular organization and poor periodicity, which do not scatter the X-ray radiation. The calculated value of the molecular tilt in PAF/DPPC 0.5/0.5 is smaller than that in the case of DPPC monolayer by ∼2.4°. It is worth highlighting that, further, even small addition of PAF into the system damages completely the periodicity of the monolayer which in consequence leads to the vanishing of the diffraction signals. Therefore, the 1:1 stoichiometry proposed in the above model is the origin of the high stability of mixed monolayer and even small addition of PAF which may change the stoichiometry leads to the loss of ordering in the surface domains.

The results obtained from GIXD measurements do not contradict the conclusions regarding the unfavorable interactions in the PAF/DPPC system drawn on the basis of thermodynamic analysis. In fact, even if the miscibility in the monolayer at the global scale is not a favorable process ($\Delta G^{Exc} > 0$), smaller domains, also observed in the BAM images, can be formed from the mixed material. This corroborates with the diffraction experiments, as it was proved that, at the molecular level, highly ordered domains of fixed stoichiometry are present at the interface.

To sum up this discussion, let us consider the implications of our results regarding natural membranes. In the undertaken experiments, we were especially focused on the possibility of introducing PAF to the cell environment exogenously; therefore, we have studied the activity of PAF in model systems in a broad range of concentration. As it was mentioned in the Introduction, both cholesterol and DPPC are very important components of the outer biomembranes' leaflet; hence, these lipids should be considered as the first target for the incorporated PAF molecules. It was proved by other authors that erythrocytes studied in vitro change their shape and undergo lysis when treated with PAF.[29] Our experiments indicate that such an effect can be connected with interactions between PAF and both membrane lipids. Considering the monolayer globally, we found that PAF exhibits a different effect depending on whether the main component of membrane is cholesterol or DPPC. Namely, on the basis of thermodynamic analysis, it turned out that, in contrast to DPPC, interactions between PAF and cholesterol in binary monolayer are energetically favorable and they are more attractive than in the case of respective pure films. Despite the character of these interactions, it was found that both investigated monolayers of pure components (cholesterol and DPPC) when treated with exogenous PAF reduce their condensation state which was shown on the basis of the calculated compressibility. On the other hand, the application of the GIXD technique enables us to obtain information regarding molecular ordering in the investigated mixed systems. It was found that, at molecular scale, PAF proved its miscibility both with Chol and DPPC. It is worth mentioning that intercalation of PAF strongly influences the molecular organization of lipids in the monolayer. The important finding is that the monolayer of DPPC can incorporate more PAF than the model membrane containing cholesterol. Namely, in the case of equimolar mixtures of PAF with the investigated membrane lipids, the system composed of PAF/Chol 0.5/0.5 does not maintain the periodicity. On the other hand, the binary equimolar system of PAF/DPPC was found to be highly ordered, whereas the 1:1 stoichiometry was recognized to be very effective in the case of monolayer periodicity retention.

Another interesting issue concerns changes of molecular tilt observed in the case of PAF/DPPC mixed films. Namely, the introduction of PAF into a monolayer of DPPC causes significant alteration of the original molecular tilt (26.8°), resulting from the structure of DPPC molecules. For mixed films, in which the molar fractions of PAF were 0.1 and 0.3, the

dx.doi.org/10.1021/jp302907e | J. Phys. Chem. B 2012, 116, 10842−10855

orientation of molecules was perpendicular to the air/water interface. On the other hand, in the case of an equimolar binary monolayer, molecules become tilted toward the NN direction with a value of 24.4°. Finally, for the higher amount of PAF, the monolayer loses its periodicity and, in consequence, no diffraction signal can be observed. These findings indicate that PAF is able to modify model membrane properties, and these changes are strongly correlated with the concentration of the investigated single-chained phospholipid.

It should be highlighted that Langmuir monolayers studied with BAM and GIXD proved their high effectiveness in studies on mimicking processes occurring in natural membranes of living organisms.

CONCLUSIONS

The aim of this contribution was to perform a detailed characteristic of the influence of platelet activating factor on the major representatives of the membrane lipids. In the comprehensive studies presented herein, we applied classical Langmuir monolayer methodology complemented with *in situ* BAM visualization, while the interactions between lipids at the molecular level were thoroughly analyzed with the application of the GIXD technique. The experiments performed in a broad range of model membrane compositions reveal that the interactions between PAF and two important components of the outer leaflet of mammalian membranes, namely, cholesterol and DPPC, are significantly different. On the basis of the Langmuir monolayer characterization, it was demonstrated that PAF mixes and consequently interacts strongly with cholesterol, but in contrast, its interactions with DPPC are thermodynamically unfavorable. Moreover, it turned out that, in the case of the PAF/DPPC binary system, phase separation is possible, especially at high surface pressure. This hypothesis found corroboration in the registered BAM images, in which it can be seen that 3D crystallites form in the monolayer of X_{PAF} = 0.3 and 0.5 compressed to a surface pressure of ∼50 mN/m. It was proved that the addition of the investigated single-chained ether phospholipid into both Chol and DPPC monolayers causes a significant decrease of monolayer condensation. Direct visualization of the investigated binary systems proves that even small amounts of PAF cause disturbance in a homogeneous monolayer of cholesterol and lead to the diminishing of the characteristic condensed domains in DPPC film. Another property, which was elucidated in this contribution, is the influence of PAF on the molecular ordering in cholesterol and DPPC monolayers. Interestingly, this problem showed a significant degree of difficulty and could be solved satisfactorily with the application of the GIXD technique. In the case of the mixed monolayer with cholesterol, PAF is able to participate in the formation of condensed highly ordered hexagonal domains only for the mixtures of $X_{PAF} \leq 0.3$, while, for the higher molar fractions of this component, the monolayer loses its periodicity and consequently the diffraction pattern cannot be obtained. In the case of PAF/DPPC, the mixed monolayer, we found a more complex situation, namely, for mixtures of X_{PAF} = 0.1 and 0.3, relatively small domains of the condensed state were found at the interface. We have registered a weak single signal, which indicates that only a small fraction of film-forming molecules are involved in the formation of a periodically ordered phase. It turns out that molecules in these binary films are oriented perpendicularly to the monolayer plane and no tilted phases were found. In the case of the GIXD results for the mixed monolayer of PAF/DPPC 0.5/0.5, a striking similarity to pure DPPC film can be seen; however, careful analysis leads to the conclusion that molecules of this system are packed in the 2D centered rectangular lattice, which implies molecular tilt toward NN. The obtained data enable us to propose a model of molecular organization in the PAF/DPPC 0.5/0.5 system, which effectively explains differences seen in the diffraction pattern.

We think that the studies presented in this paper are valuable in the sense of a better understanding of the physiological significance of PAF. As it was proved in previous articles, based mainly on biochemical studies, this representative of single-chained ether phospholipids is characterized by a strong activity in membrane environment. Despite this, until now the correlation between the PAF impact on membrane components like cholesterol and DPPC and its mechanism of action has not been proposed. Therefore, our intention was to open a discussion on this issue. Certainly, the presented results provide new facts regarding the properties of PAF in the model systems imitating biomembranes; however, to obtain a broader view on this problem, future studies on other structurally similar single-chained phospholipids in more complex systems should be undertaken.

ASSOCIATED CONTENT

Supporting Information

BAM images registered for a monolayer of PAF, cholesterol, as well as binary monolayer of PAF/cholesterol in the broad range of molar fractions. Intensity vs out-of-plane scattering vector Q_z (Bragg rods) measured for all of the investigated monolayers. This material is available free of charge via the Internet at http://pubs.acs.org.

AUTHOR INFORMATION

Corresponding Author

*E-mail: flasinsk@chemia.uj.edu.pl. Phone: +48 012 663 20 82. Fax: +48 012 634 05 15.

Notes

The authors declare no competing financial interest.

ACKNOWLEDGMENTS

This project was financed by the National Science Centre (No. DEC-2011/01/B/ST4/00910). We gratefully acknowledge HASYLAB, DESY (Hamburg) for granting us beamtime at the BW1 beamline and would like to express our gratitude to Dr Bernd Struth for his help at BW1. The research was carried out with the equipment (UltraBAM) purchased thanks to the financial support of the European Regional Development Fund in the framework of the Polish Innovation Economy Operational Program (Contract No. POIG.02.01.00-12-023/08). We would like to express our gratitude to Stefan Schneider and his colleagues (Accurion GmbH) for their help in BAM image processing.

REFERENCES

(1) *Metabolism and function of bioactive ether lipids in brain*; Farooqui, A. A., Farooqui, T., Horrocks, L. A., Eds.; Springer: New York, 2008.
(2) Magnusson, C. D.; Haraldsson, G. D. *Chem. Phys. Lipids* **2011**, *164*, 315.
(3) Benveniste, J.; Henson, P. M.; Cochrane, C. G. *J. Exp. Med.* **1972**, *136*, 1356.
(4) Heymans, F.; Michel, E.; Borrel, M. C.; Wichrowski, B.; Godfroid, J. J.; Convert, O.; Coeffier, E.; Tence, M.; Benveniste, J. *Biochim. Biophys. Acta* **1981**, *666*, 230.

(5) Demopoulos, C. A.; Pinckard, R. N.; Hanahan, D. J. *J. Biol. Chem.* **1979**, *254*, 9355.
(6) McManus, L. M.; Pinckard, R. N. *Crit. Rev. Oral Biol. Med.* **2000**, *11*, 240.
(7) Chen, J.; Yang, L.; Foulks, J. M.; Weyrich, A. S.; Marathe, G. K.; McIntyre, T. M. *J. Lipid Res.* **2007**, *48*, 2365.
(8) Dyer, K. D.; Percopo, C. M.; Xie, Z.; Yang, Z.; Kim, J. D.; Davoine, F.; Lacy, P.; Druey, K. M.; Moqbel, R.; Rosenberg, H. F. *J. Immunol.* **2010**, *184*, 6327.
(9) Bussolino, F.; Camussi, G.; Aglietta, M.; Braqeut, P.; Bosia, A; Pescarmona, G.; Sanavio, F.; D'Urso, N.; Marchisio, P. C. *J. Immunol.* **1987**, *139*, 2439.
(10) Zhu, L.; He, P. *Am. J. Physiol. Heart Circ. Physiol.* **2005**, *288*, H2869.
(11) Knezevic, I. I.; Predescu, S. A.; Neamu, R. F.; Gorovoy, M. S.; Knezevic, N. M.; Easington, C.; Malik, A. B.; Predescu, D. N. *J. Biol. Chem.* **2009**, *284*, 5381.
(12) Kantar, A.; Giorgi, P. L.; Fiorini, R. *Agents Actions* **1993**, *38*, C115.
(13) Göggel, R.; Uhlig, S. *Eur. Respir. J.* **2005**, *25*, 849.
(14) Qu, X. W.; Rozenfeld, R. A.; Huang, W.; Crawford, S. E.; Gonzalez, C. F.; Hsueh, W. *J. Physiol.* **1998**, *512*, 227.
(15) Kuebler, W. M.; Yang, Y.; Samapati, R.; Uhlig, S. *Cell. Physiol. Biochem.* **2010**, *26*, 29.
(16) Ferreira, M. A. N. D.; Barcelos, L. S.; Teixeira, M. M.; Bakhle, Y. S.; Andrade, S. P. *Life Sci.* **2007**, *81*, 210.
(17) Denizot, Y.; Gainant, A.; Guglielmi, L.; Bouvier, S.; Cubertafond, P.; Mathonnet, M. *Oncogene* **2003**, *22*, 7222.
(18) Melnikova, V.; Bar-Eli, M. *Cancer Metastasis Rev.* **2007**, *26*, 359.
(19) Braeuer, R. R.; Zigler, M.; Villares, G. J.; Dobroff, A. S.; Bar-Eli, M. *Semin. Cancer Biol.* **2011**, *21*, 83.
(20) Denizot, Y.; Chianea, T.; Labrousse, F.; Truffinet, V.; Delage, M.; Mathonnet, M. *Eur. J. Endocrinol.* **2005**, *153*, 31.
(21) Tsoukatos, D. C.; Brocheriou, I.; Moussis, V.; Panopoulou, C. P.; Christofidou, E. D.; Koussissis, S.; Sismanidis, S.; Ninio, E.; Siminelakis, S. *J. Lipid Res.* **2008**, *49*, 2240.
(22) De Faire, U.; Frostegard, J. *Ann. N.Y. Acad. Sci.* **2009**, *1173*, 292.
(23) Montrucchio, G.; Alloatti, G.; Camussi, G. *Physiol. Rev.* **2000**, *80*, 1669.
(24) Saougos, V. G.; Tambaki, A. P.; Kologirou, M.; Kostapanos, M.; Gazi, I. F.; Wolfert, R. L.; Elisaf, M.; Tselepis, A. D. *Arterioscler., Thromb., Vasc. Biol.* **2007**, *27*, 2236.
(25) Poisson, C.; Rollin, S.; Véronneau, S.; Bousquet, S. M.; Larrivée, J.-F.; Le Gouill, C.; Boulay, G.; Stankova, J.; Rola-Pleszczynski, M. *J. Immunol.* **2009**, *183*, 2747.
(26) McIntyre, T. M.; Prescott, S. M.; Stafforini, D. M. *J. Lipid Res.* **2009**, *50*, S255.
(27) Liu, J.; Chen, R.; Marathe, G. K.; Febbraio, M.; Zou, W.; McIntyre, T. M. *Circ. Res.* **2011**, *108*, 469.
(28) Isomaa, B.; Hagerstrand, H.; Paatero, G. *Biochim. Biophys. Acta* **1987**, *899*, 930.
(29) Mrówczyńska, L.; Hägerstrand, H. *J. Biochem. Mol. Toxicol.* **2009**, *23*, 345.
(30) Schneider, E.; Haest, C. W. M.; Deuticke, B. *FEBS Lett.* **1986**, *198*, 311.
(31) Brewer, C.; Bonin, F.; Bullock, P.; Nault, M. C.; Morin, J.; Imbeault, S.; Shen, T. Y.; Franks, D. J.; Bennett, S. A. L. *J. Neurochem.* **2002**, *82*, 1502.
(32) Stafforini, D. M.; Rollins, E. N.; Prescott, S. M.; McIntyre, T. M. *J. Biol. Chem.* **1993**, *268*, 3857.
(33) Hąc-Wydro, K.; Dynarowicz-Łątka, P. *Colloids Surf., B* **2010**, *81*, 492.
(34) McConnell, H, M.; Radhakrishnan, A. *Biochim. Biophys. Acta* **2003**, *1610*, 159.
(35) Grosman, N. *Int. Immunopharmacol.* **2001**, *1*, 1321.
(36) Bonin, F.; Ryan, S. D.; Migahed, L.; Mo, F.; Lallier, J.; Franks, D. J.; Arai, H.; Bennett, S. A. L. *J. Biol. Chem.* **2004**, *279*, 52425.
(37) Kjaer, K. *Physica B* **1994**, *198*, 100.
(38) Als-Nielsen, J.; Jacquemain, D.; Kjaer, K.; Leveiller, F.; Lahav, M.; Leiserovitz, L. *Phys. Rep.* **1994**, *246*, 251.
(39) Jensen, T. R.; Balashev, K.; Bjornholm, T.; Kjaer, K. *Biochemie* **2001**, *83*, 399.
(40) Kuzmenko, I.; Rapaport, H.; Kjaer, K.; Als-Nielsen, J.; Weissbuch, I.; Lahav, M.; Leiserowitz, L. *Chem. Rev.* **2001**, *101*, 1659.
(41) Davies, J. T.; Rideal, E. K. *Interfacial Phenomena*; Academic Press: New York and London, 1963.
(42) Gains, G. L. *Insoluble monolayers at liquid/gas interfaces*; Wiley-Interscience: New York, 1966.
(43) *Modern characterization methods of surfactant systems*; Binks, B. P., Ed.; Marcel Dekker, Inc.: New York, 1999.
(44) *Novel method to study interfacial layers*; Möbius, D., Miller, R., Eds.; Elsevier: Amsterdam, 2001.
(45) Dynarowicz-Łątka, P.; Hąc-Wydro, K. *Colloids Surf., B* **2004**, *37*, 21.
(46) Seoane, R.; Miñones, J.; Conde, O.; Miñones, J., Jr. *Colloids Surf., A* **2000**, *174*, 329.
(47) Wydro, P.; Hąc-Wydro, K. *J. Phys. Chem. B* **2007**, *111*, 2495.
(48) Flasiński, M.; Broniatowski, M.; Wydro, P.; Dynarowicz-Łątka, P. *J. Phys. Chem. B* **2012**, *116* (10), 3155.
(49) Feng, S.-S. *Langmuir* **1999**, *15*, 998.
(50) Flasiński, M.; Broniatowski, M.; Majewski, J.; Dynarowicz-Łątka, P. *J. Colloid Interface Sci.* **2010**, *348*, 511.
(51) Rapaport, H.; Kuzienko, I.; Lafont, S.; Kjaer, K.; Howes, P. B.; Als-Nielsen, J.; Lahav, M.; Leiserovitz, L. *Biophys. J.* **2001**, *81*, 2729.
(52) Scheffer, L.; Solomonov, I.; Weygand, M. J.; Kjaer, K.; Leiserovitz, L.; Addadi, L. *Biophys. J.* **2005**, *88*, 3381.
(53) Ratajczak, M. K.; Chi, E. Y.; Frey, S. L.; Cao, K. D.; Luther, L. M.; Lee, K. Y. C. *Phys. Rev. Lett.* **2009**, *103*, 028103.
(54) Gong, K.; Feng, S.-S.; Go, M. L.; Soew, P. H. *Colloids Surf., A* **2002**, *207*, 113.
(55) Weidemann, G.; Vollhardt, D. *Colloids Surf., A* **1995**, *100*, 187.
(56) Miñones, J., Jr.; Rodriguez-Patino, J. M.; Conde, O.; Carrera, C.; Seoane, R. *Colloids Surf., A* **2002**, *203*, 273.
(57) Hąc-Wydro, K.; Flasiński, M.; Broniatowski, M.; Dynarowicz-Łątka, P.; Majewski, J. *J. Colloid Interface Sci.* **2011**, *364*, 133.
(58) Brezesinski, G.; Dietrich, A.; Struth, B.; Böhm, C.; Bouwman, W. G.; Kjaer, K.; Möhwald, H. *Chem. Phys. Lipids* **1995**, *76*, 145.
(59) Aroti, A.; Leontidis, E.; Maltseva, E.; Brezesinski, G. *J. Phys. Chem. B* **2004**, *108*, 15238.
(60) Wiegart, L.; Struth, B.; Tolan, M.; Terech, P. *Langmuir* **2005**, *21*, 7349.
(61) Bringezu, F.; Majerowicz, M.; Wen, S.; Reuther, G.; Tan, K. T.; Kuhlmann, J.; Waldmann, H.; Huster, D. *Eur. Biophys. J.* **2007**, *36*, 491.
(62) Kaganer, V. M.; Möhwald, H.; Dutta, P. *Rev. Mod. Phys.* **1999**, *71*, 779.